Korean J. Chem. Eng., **28**(8), 1693-1697 (2011)
DOI: 10.1007/s11814-011-0021-9

Photodegradation of benzene, toluene, ethylbenzene and xylene by fluidized bed gaseous reactor with TiO_2/SiO_2 photocatalysts

Jae-Hyoung Park, Yong-Su Seo, Hyun-Seung Kim, and Il-Kyu Kim†

Department of Environmental Engineering, Pukyong National University, 599-1, Daeyeon-dong, Nam-gu, Busan 608-737, Korea
(*Received 21 June 2010 • accepted 24 January 2011*)

Abstract−The photodegradation of BTEX (benzene, toluene, ethylbenzene and xylene) in a photocatalytic fluidized bed reactor with TiO_2/SiO_2 was investigated. The TiO_2 film was prepared using the sol-gel method and coated onto silica-gel powder. The effects of the superficial gas velocity and SiO_2 size on the photodegradation of BTEX were examined in a fluidized bed reactor. At steady-state operation, above 79, 79, 99, 98, and 98% removal efficiencies were achieved for benzene, toluene, ethylbenzene, m, p-xylene and o-xylene, respectively, under optimal conditions (2.0 U_{mf} of superficial gas velocity and 1.43 of height/diameter ratio). The reaction product such as CO_2 was detected and intermediate products such as benzaldehyde, malonic acid, acetaldehyde, and formic acid were identified from the photocatalytic reaction. Also, small amounts of benzoic acid and benzyl alcohol were found through analyzing the intermediate species adsorbed on the photocatalysts. The experimental results can lead to the development of an efficient photocatalytic treatment system that utilizes solar energy and TiO_2/SiO_2 photocatalysts.

Key words: BTEX, Photocatalytic Fluidized Bed Reactor, TiO_2/SiO_2, Photodegradation

INTRODUCTION

Volatile organic compounds (VOCs) are important air pollutants that are usually found in the atmosphere of all urban and industrial areas. Emission of VOCs with vapor pressure above 10^{-3} mmHg has become a very serious problem to public health, for which several countries have implemented emission control measures. Many VOCs are known to be toxic and considered to be carcinogenic. In particular, many studies on chemical detoxification and pollutant degradation have focused on the removal of toxic and hazardous substances, including benzene, toluene, ethyl benzene and xylene (BTEX). Especially, toluene is a typical VOC and major indoor and industrial air pollutant [1]. This toxic compound is widely used as a solvent in organic chemistry and industry. For air purification, various studies have been carried out using gas phase photocatalytic degradation for the removal of BTEX and other air pollutants.

Pollution by VOCs has prompted the need for an intensive search for the best available technology (BAT) for their control and removal. The application of activated carbon adsorption systems has emerged and been verified as one of the most effective technologies for the removal of VOCs compared with impractical, traditional methods (e.g., flocculation, sedimentation and filtration) [2]. However, activated carbon is recognized as an expensive material in many countries, and is a non-destruction technology, which can cause a secondary pollution problem. Moreover, the efficiency of condensation and bio-filtration are limited, whereas incineration has good decomposition efficiency but requires high construction and operation costs with high energy consumption Thus, an alternative technology needs to be found that can degrade BTEX to either make less harmful intermediates or lead to their complete mineralization.

Advanced oxidation processes (AOPs) are particularly promising technologies, defined as processes that involve the generation of hydroxyl radicals in sufficient amounts to enhance water and air purification. AOPs can generally compromise various combination methods with oxidation agents, irradiation and catalysts in order to generate the hydroxyl radicals. The TiO_2/UV method is a well known AOP. The TiO_2/SiO_2 method, called photo-catalytic oxidation, utilizes positive holes and electrons produced on an irradiated semiconductor catalyst surface. As a photocatalyst, TiO_2 is known for its low cost, biocompatibility and non-toxicity [3].

Heterogeneous photocatalytic purification of gaseous organic pollutants has been studied extensively in the past decade [2-8,10,12]. However, to increase the reaction rate of the photocatalytic oxidation in the gas-solid heterogeneous photocatalysis, the reaction system must provide efficient continuous contact of ultraviolet photons with photocatalysts and gaseous reactants. A fluidized bed is known as a good chemical reactor due to excellent reactants contact, high mass and heat transfer rate and easy to control reactor temperature. It is believed that a fluidized bed can take advantage of better use of light, ease of temperature control, and good contacting between target compounds and photocatalysts over a fluidized bed system.

In this study, the photodegradation of BTEX was examined using a fluidized bed gaseous reactor. The effects of important parameters, such as initial concentration, superficial gas velocity and photocatalysts sizes, on the photodegradation of BTEX were examined. And identification of reaction and intermediate products during the photodegradation of BTEX has been implemented. This fundamental information obtained from the experiments can be used for the development of a destructive, cost-effective, and clean treatment

†To whom correspondence should be addressed.
E-mail: ikkim@pknu.ac.kr

process for VOCs.

MATERIALS AND METHODS

1. Preparation TiO_2/SiO_2 Photocatalyst

Silica gel (particle diameter=40-63 μm; surface area=561 m^2/g, Merck) was used as a substrate to improve the fluidization performance of the TiO_2 particles, since TiO_2 powder is classified as Geldart C Group, which means it has poor fluidization characteristics. Precursor solutions for TiO_2 coating onto the silica gel were prepared using tetraisopropoxide (98.0% Junsei Chemical, Japan), hydrochloric acid (36%, Junsei Chemical Co., Ltd., Japan), isopropyl alcohol (for ACS analysis, Carlo Erba Reagenti) and deionized water. The details for the photocatalyst preparation are shown in Fig. 1.

After this solution was mixed for 180 minutes at room temperature, the silica gel was added to the colloidal suspensions of TiO_2, dried at 100 °C for 24 hours, and calcinated at 500 °C for 1 hour.

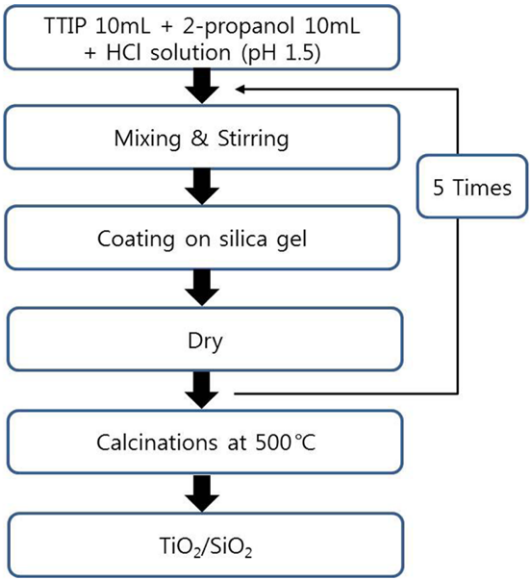

Fig. 1. Procedure to prepare TiO_2/SiO_2 photocatalysts.

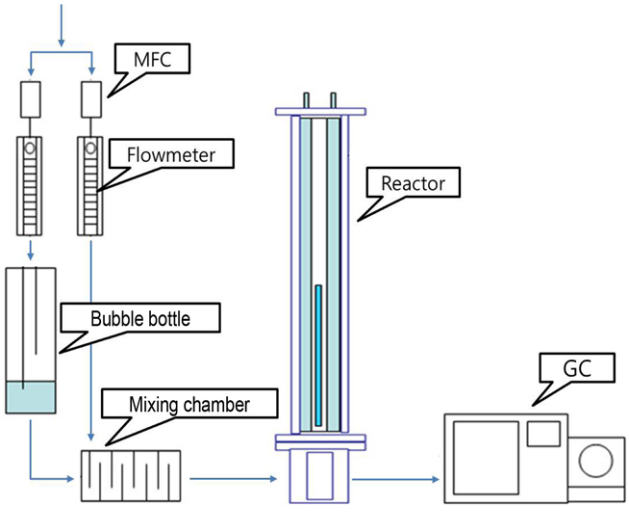

Fig. 2. Schematic diagram of the annulus photocatalytic gaseous system.

2. Fluidized Bed Photoreactor

The basic experimental setup is shown in Fig. 2. A small Pyrex glass tube (60 mm O.D.×1,000 mm Height) was located in the middle of a large Pyrex glass tube (70 mm O.D.×1,000 mm Height). A gas distributor was also used to provide a gas stream for uniform fluidization of the TiO_2/SiO_2 photocatalyst. A UV lamp (Philips, F15TBLB, Ultraviolet Output=2.6 watt, Ultraviolet rays range; 315-400 nm, Ultraviolet rays peak; 352 nm, 368 nm) was installed inside the small Pyrex tube for effective ultraviolet light irradiation.

The system used in this study consisted of a BTEX feeding device (bubble bottle and canister, TO-Can™ 15 L, Restek Co., Ltd., UK), a photocatalytic fluidized bed gaseous reactor and a detector. BTEX gases were prepared by mixing air and VOCs through a glass saturator and canister. High and low concentrations were initially prepared at 100±5 ppmv and 100±5 ppbv by the addition of air to the mixing chamber. To distinguish the BTEX removal by adsorption on the surface of photocatalyst, the system had been running idle with the UV lamp turned off until it reached the steady state condition.

The minimum fluidization velocity (U_{mf}) of the TiO_2/SiO_2 photocatalyst was determined from the pressure drop and the expanded bed height in the reactor on varying the superficial gas velocity (U_g). The BTEX was analyzed by gas chromatograph (QP2010, Shimadzu., Japan) equipped with a flame ionization detector and mass spectrometer, which was interlocked with an automatic thermal desorption System (ATD400, Perkin Elmer., USA). The measurement system included highly purified N_2 as the carrier gas and an AT1 column.

3. Analytical Methods

To identify the gaseous reaction products in the outlet of the photocatalytic reactor, the gaseous sample was collected using a Tedler bag and led to GC/MS directly with a gaseous syringe. During degradation of pollutants, the color of photocatalysts changed to yellow. To identify the yellow substances (intermediate products) on the surfaces of photocatalysts, a solvent of methanol was used to extract the intermediate products on the surfaces. Then, the extracted sample was analyzed with GC/MS.

RESULTS AND DISCUSSION

1. Characterization of TiO_2/SiO_2

Structural characterization was carried out by XRD to verify the effects of hydrothermal treatments on the crystallographic structure and crystallite size of the TiO_2/SiO_2. The TiO_2/SiO_2 photocatalysts were made using a sol-gel method and calcinated at 500 °C for 1 hour.

Fig. 3 shows the SEM images of the 60-mesh TiO_2/SiO_2 photocatalyst surface. The crystalline phase of the prepared TiO_2/SiO_2 was analyzed using powder X-ray diffraction analysis (XRD, Philip Pw 1710), with nickel filtered CuKa radiation (30 kV, 40 mA), a 2θ range from 5 to 80 degrees, scan speed of 10° min^{-1} and time constant of 1 sec.

Fig. 4 shows the XRD pattern of the synthesized TiO_2/SiO_2. The broad diffraction lines of anatase are located in 25.3°, 37.8°, 47.9°, 54.0°, 55.4° and 62.9° (Table 1).

The dominant anatase structures of the TiO_2/SiO_2 particles were observed after calcinating the TiO_2/SiO_2 at 500 °C for 1 hour. In sev-

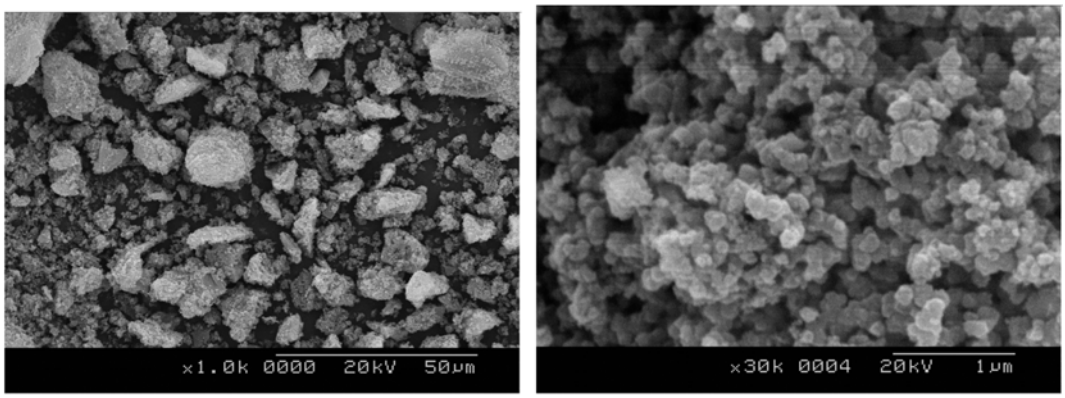

(a) Surface of TiO_2/SiO_2 (x1,000) (b) Surface of TiO_2/SiO_2 (x30,000)

Fig. 3. SEM images of the prepared TiO_2/SiO_2 photocatalysts.

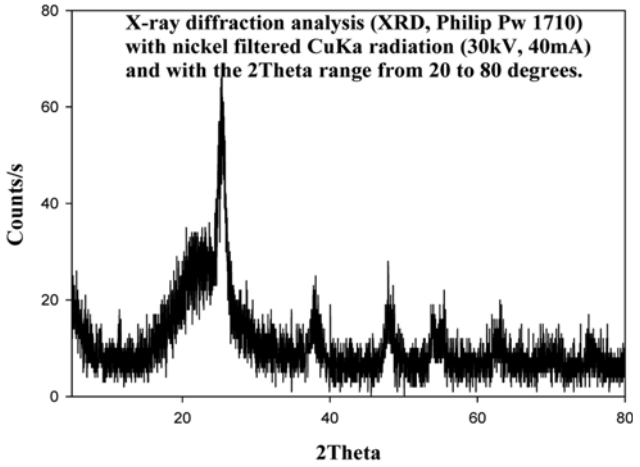

Fig. 4. The result from XRD.

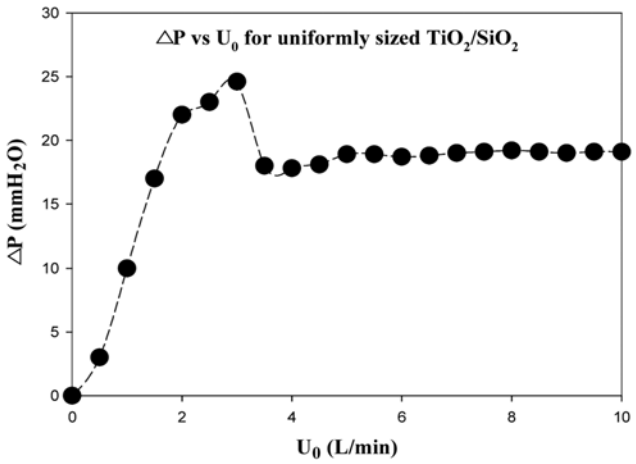

Fig. 5. Minimum fluidization velocity.

eral previous articles [5], anatase has shown much better photocatalytic activity than the rutile form.

The different characteristics between the rutile and anatase forms were attributed to the different positions of the conduction band (more positive for rutile) and to the higher recombination rate of electron-hole pairs in the rutile form.

2. Minimum Fluidization Velocity and Superficial Gas Velocity of TiO_2/SiO_2 Photocatalyst

The minimum fluidization velocity (U_{mf}) in the TiO_2/SiO_2 photocatalytic reactor is shown Fig. 5. When the expanded bed height reached a maximum value, the flow rate was measured as 3.00 $Lmin^{-1}$. As a result, a minimum fluidization velocity of 2.74 $Lmin^{-1}$ was obtained.

Fig. 6 shows the effect of U_g/U_{mf} on the removal of BTEX in the fluidized bed system, which was shown to increase when U_g/U_{mf}, reached a maximum, at U_g/U_{mf}=2.0, and then decreased with further increases in U_g/U_{mf}. The enhancement of BTEX removal efficiency below the optimal U_g/U_{mf} value appeared to be caused by the

Table 1. The identified anatase peak list

d-Spacing (Å)	Relative intensity (%)	Angle (°2 Theta)	Peak height (counts/s)	Background (counts/s)	Tip width (°2 Theta)	Significance
3.51843	100.00	25.29206	126.76	74.21	0.32000	0.70
2.37915	22.66	37.78132	28.72	25.77	0.64000	0.82
1.89791	28.83	47.88970	36.54	22.72	0.96000	2.59
1.69722	18.51	53.98170	23.46	21.15	0.40000	0.65
1.65588	26.80	55.44365	33.97	21.29	0.20000	0.73
1.47611	22.93	62.91043	29.07	33.91	0.10000	100.00
1.36232	10.17	68.86282	12.89	25.11	0.10000	100.00
1.26762	6.23	74.84104	7.90	20.92	0.80000	0.70

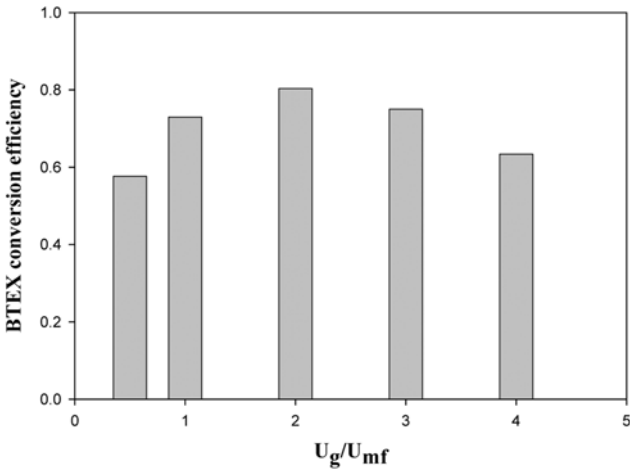

Fig. 6. Effect of U_g/U_{mf} on BTEX conversion (UV light intensity: 3 mW/cm^2, U_{mf}: 2.0, Initial concentration: 100±5 ppmv).

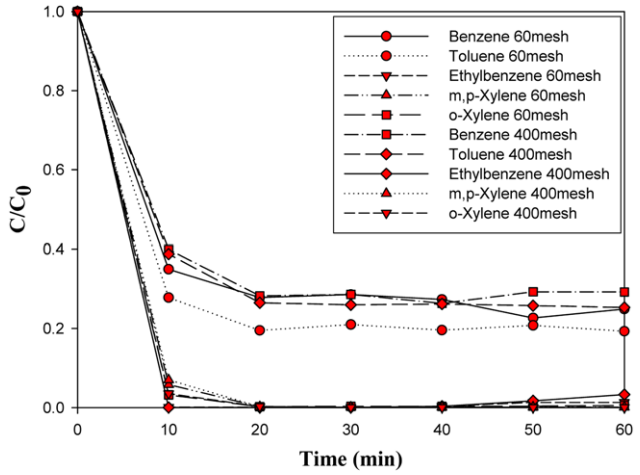

Fig. 8. Photodegradation of BTEX by the fluidized bed gaseous reactor with different sizes of TiO_2/SiO_2 photocatalysts (BTEX initial concentration: 100±5 ppmv, 60-mesh and 400-mesh photocatalysts, RH: 0%).

increased contact between UV light and the photocatalysts because UV light can irradiate more TiO_2/SiO_2 particles with increasing U_g/U_{mf}.

The BTEX removal efficiency was not as a function of the annulus gap under fixed bed conditions. The optimal annulus gap for the maximum BTEX removal efficiency was found to be 8 mm at an U_g/U_{mf}=2.0. Therefore, in this study, an annulus gap of 8 mm was fixed for all other experimental conditions. The optimal annulus gap changed to higher values due to the increased bubble size, and eventually touched both sides of the photoreactor walls with increasing U_g. In a previous study, the annulus gap was found to be an important parameter governing the appropriate bubble size for light transmission to the increase removal efficiency over the TiO_2/SiO_2 photocatalyst [6].

3. Effect of Sole UV on BTEX Removal

The effect of UV light on the removal efficiency without the TiO_2/SiO_2 photocatalyst is shown in Fig. 7. When the initial concentration of BTEX was 100±5 ppmv, benzene was not removed by UV light alone. The toluene removal efficiency exhibited an almost constant rate at about 1.2%, while those of ethylbenzene, m, p-xylene and o-xylene were about 4.8, 3.6 and 5.3%, respectively. When the concentrations of BTEX were maintained at 100±5 ppbv, benzene was also not removed. The toluene removal efficiency remained almost constant at about 4.6%, while those of ethylbenzene, m, p-xylene and o-xylene were about 7.6, 7.2 and 8.7%, respectively.

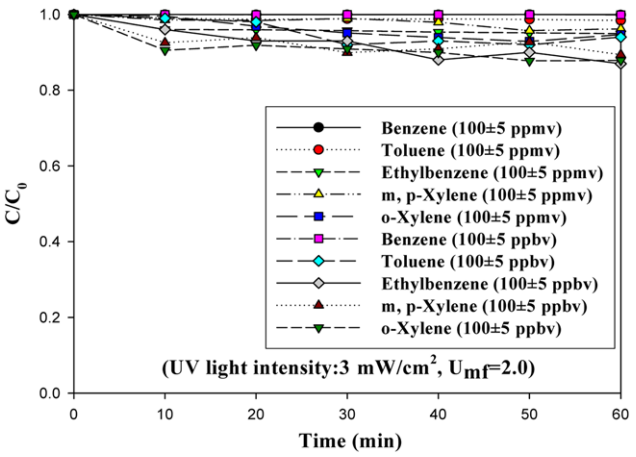

Fig. 7. Effect of UV without photocatalysts on BTEX conversion (UV light intensity: 3 mW/cm^2, U_{mf}: 2.0, Initial concentration: 100±5 ppmv and 100±5 ppbv).

4. BTEX Removal Efficiency with TiO_2/SiO_2

The results for BTEX decomposition under UV irradiation with the TiO_2/SiO_2 photocatalyst are shown in Fig. 8. As shown, the removal of BTEX rapidly increased within an operation time of 10 minutes.

The removal efficiencies of benzene, toluene, ethylbenzene, m, p-xylene and o-xylene with 60-mesh TiO_2/SiO_2 photocatalysts were 76.3, 78.4, 99.6, 99.8 and 99.9%, respectively. The BTEX initial concentration was set at 100±5 ppmv, with the relative humidity (RH) maintained at 0%.

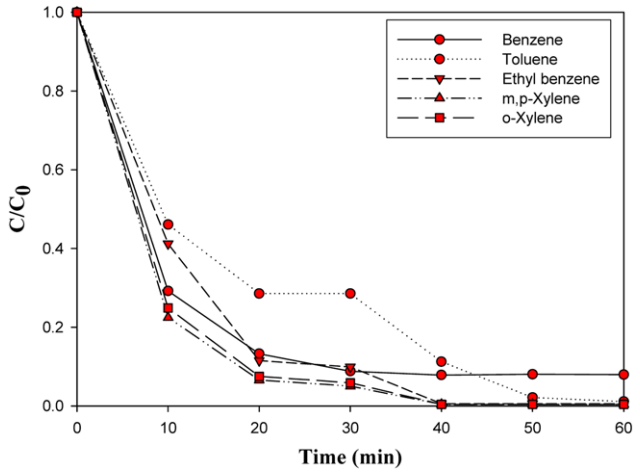

Fig. 9. Photodegradation of BTEX by the fluidized bed gaseous reactor with 60-mesh TiO_2/SiO_2 photocatalysts (BTEX initial concentration: 100±5 ppbv, 60-mesh photocatalyst, RH: 0%).

In addition, when the concentrations of BTEX were maintained 100±5 ppmv, the benzene removal efficiency with 400-mesh TiO_2/SiO_2 photocatalyst remained at a constant value of around 75%, while those of toluene, ethylbenzene, m, p-xylene and o-xylene were about 79.9, 99.4, 98.0 and 98.3%, respectively.

As shown in Fig. 9, the removal efficiencies of benzene, toluene, ethylbenzene, m, p-xylene, and o-xylene with 60-mesh TiO_2/SiO_2 photocatalysts of 87.5, 80.4, 89.2, 94.2 and 93.4%, respectively, were achieved with an initial BTEX concentration of 100±5 ppbv and RH of 0%.

As shown in Fig. 8, the 60-mesh TiO_2/SiO_2 photocatalyst was more efficient than the 400-mesh photocatalyst for the removal of BTEX because the finer photocatalysts (400-mesh TiO_2/SiO_2) were not sufficiently fluidized by the gas flow (bubbles are not created inside the fluidized bed reactor). Therefore, the fluidization requires an optimal photocatalyst size.

5. Identification of Reaction and Intermediate Products

The photocatalyst deactivation is caused by the strong adsorption of reaction and intermediate products generated during photodegradation of air contaminants. In this system, a reaction product such as CO_2 was detected and intermediate products such as benzaldehyde, malonic acid, acetaldehyde, and formic acid were identified. Also, small amount of benzoic acid and benzyl alcohol was found through analyzing the intermediate species adsorbed on the photocatalysts.

The photodegradation is brought about by OH radicals and positive holes. The radicals and positive holes can react with BTEX on the surface of photocatalysts. A proposed reaction pathway describing the photodegradation mechanism in gas phase can be suggested; the degradation is started by the OH radical addition to VOCs, which yield benzaldehyde. The subsequent cleavage of the benzaldehyde would result in the formation of malonic acid. The malonic acid is converted to lower molecular weight organic compounds such as formic acid and acetaldehyde. The formic acid and acetaldehyde will then be converted to carbon dioxide and H_2O as the end products through the subsequent reaction steps. Eventually, the reaction mineralizes these VOCs to end products such as carbon dioxide and H_2O.

CONCLUSIONS

The photocatalytic degradation characteristics of BTEX have been studied in an annulus fluidized bed system, with TiO_2 coated onto SiO_2. Our conclusions are as follows.

1. The best experimental conditions of U_g and U_{mf} based on the maximum BTEX removal efficiencies were 2.0 and 1.43, respectively, for the bed height/diameter ratio. Under steady-state operation (using 60-mesh photocatalyst), a BTEX initial concentration of 100±5 ppmv and RH of 0%, about 76.3, 78.4, 99.6, 99.8 and 99.9% removal efficiencies were achieved for benzene, toluene, ethylbenzene, m, p-xylene and o-xylene, respectively.

The removal efficiencies with 60-mesh TiO_2/SiO_2 photocatalysts of 87.5, 80.4, 89.2, 94.2 and 93.4% were achieved for benzene, toluene, ethylbenzene, m, p-xylene and o-xylene, respectively, with an initial BTEX concentration of 100±5 ppbv and RH of 0%.

2. The 60-mesh TiO_2/SiO_2 photocatalyst was more efficient than the 400-mesh photocatalyst for the removal of BTEX due to the finer photocatalyst (400-mesh TiO_2/SiO_2) being scattered by the gas flow; therefore, the fluidization requires an optimal photocatalyst size.

3. In this system, a reaction product such as CO_2 was detected and intermediate products such as benzaldehyde, malonic acid, acetaldehyde, and formic acid were identified. Also, small amounts of benzoic acid and benzyl alcohol were found through analyzing the intermediate species adsorbed on the surface of photocatalysts.

In conclusion, the fundamental information obtained from this study can be used for the development of an efficient and practical AOP system which utilizes solar energy and TiO_2/SiO_2 photocatalysts.

ACKNOWLEDGEMENT

This research work was supported by the Korea Meteorological Administration Research and Development Program under Grant CATER 2007-4403.

REFERENCES

1. A. H. AM Daifullah and M. M. Mohamed, *J. Chem. Technol. Biotechnol.*, **26**, 468 (2004).
2. A. Nakajima, H. Obata, Y. Kaneshima and K. Okada, *Catal. Commun*., **6**, 716 (2005).
3. K. Sunada, T. Watanabe, K. Hashimoto and A. Fujishima, *Environ. Sci. Technol*., **32**, 726 (1998).
4. M. Keshmiri, T. Troczynski and M. Mohseni, *J. Hazard. Mater*., **B218**, 130 (2006).
5. T. H. Lim, S. M. Jeong, S. D. Kim and G. Janos, *J. Photochem. Photobiol. A: Chem*., **134**, 209 (2000a).
6. A. Strini, S. Cassese and L. Schiavi, *Appl. Catal. B, Environ*., **61**, 90 (2005).
7. V. Auguliaro, S. Coluccia, V. Loddo, L. Marchese, G. Martra, L. Palmisano and M. Schiavello, *Appl. Catal. B: Environ.*, **20**, 15 (1999).
8. S. W. Kim, M. S. Kang and S. J. Choung, *J. Ind. Eng. Chem*., **11**(3), 416 (2005).
9. I. K. Kim, S. J. Yoa, J. K. Lee and C. P. Huang, *Korean J. Chem. Eng*., **20**(6), 1045 (2003).
10. I. K. Kim, H. J. Ha, S. K. Lee and J. K. Lee, *Korean J. Chem. Eng*., **22**(3), 382 (2005).
11. A. Sclafani and J. M. Herrmann, *J. Phys. Chem*., **100**, 13655 (1996).
12. S. K. Dolberg, *Air. J. Air Waste Manage. Assoc.*, **46**, 891 (1996).